J Mol Model (2013) 19:3501–3506
DOI 10.1007/s00894-013-1882-0

ORIGINAL PAPER

Reaction mechanism of $CH_3M{\equiv}MCH_3$ (M=C, Si, Ge) with C_2H_4: [2+1] or [2+2] cycloaddition?

Suhong Huo · Xiaoyan Li · Yanli Zeng · Shijun Zheng · Lingpeng Meng

Received: 8 January 2013 / Accepted: 5 May 2013 / Published online: 26 May 2013

Abstract The mechanism of the cycloaddition reaction $CH_3M{\equiv}MCH_3$ (M=C, Si, Ge) with C_2H_4 has been studied at the CCSD(T)/6-311++G(d,p)//MP2/6-311++G(d,p) level. Vibrational analysis and intrinsic reaction coordinate (IRC), calculated at the same level, have been applied to validate the connection of the stationary points. The breakage and formation of the chemical bonds of the titled reactions are discussed by the topological analysis of electron density. The calculated results show that, of the three titled reactions, the $CH_3Si{\equiv}SiCH_3+C_2H_4$ reaction has the highest reaction activity because it has the lowest energy barriers and the products with the lowest energy. The $CH_3C{\equiv}CCH_3+C_2H_4$ reaction occurs only with difficulty since it has the highest energy barriers. The reaction mechanisms of the title reactions are similar. A three-membered-ring is initially formed, and then it changed to a four-membered-ring structure. This means that these reactions involve a [2+1] cycloaddition as the initial step, instead of a direct [2+2] cycloaddition.

Keywords Cycloaddition · Heavier group 14 element · Reaction mechanism · Topological analysis of electron density

Introduction

Heavier group 14 element alkyne analogues have been a focus of theoretical and experimental interest since the early 1980s [1-18]. The synthesis, isolation, and characterization of the first stable heavier diterel alkyne analogues have been reported only since 2000 [18-26]. The first discovery of a stable heavier group 14 element analogue of an alkyne was Ar*PbPbAr* (Ar*=C_6H_3-2,6(C_6H_2-2,4,6-Pr^i_3)$_2$, which was synthesized by Power and his coworkers in 2000 [19]. Then, in 2002, they prepared stable Ge [26] and Sn [20] alkyne analogues using more careful control of the reaction conditions and stoichiometry. Subsequent work by Sekiguchi [22] and Mayer [25] afforded the first stable disilynes in 2004 by reduction of 1,2-dihalogendisilyl precursors. In all cases, the data show that the heavier main-group elements have fundamentally different electronic properties from their lighter congeners [1, 27]. The heavier group 14 element alkyne analogues have a trans-bent, planar core arrangement, in which the trans-bending increases in the sequence of C, Si and Ge. Recently, Nagase examined the reactivity of "disilyne" toward π-bonds [28] and Power *et al.* showed that the "digermyne" can react readily with unsaturated molecules, such as alkynes and azides, under ambient conditions [29, 30]. Pilling [31] and Piecuch [32] determined the mechanism of cyclopentyne-alkene and cyclopentyne-ethylene cyclopentyne belong to [2+2] cycloaddition, while Nagase determined it belongs to [2+1] cycloaddition [28]. To date, although a few papers have described the cycloaddition reaction of the disilyne RSi≡SiR (R=organic subsituent) with alkenes, and four-numbered-ring structure exist in the products [21, 30]. While how the four-numbered-ring structures forms and the reactivity of other group 14 element alkyne analogues is much less known, therefore, a comparison of chemical behavior of heavier group 14 element alkyne analogues with that of alkynes is of special interest, and a detailed knowledge of the cycloaddition reaction mechanism is very desirable.

In this paper, we report theoretical studies of the cycloaddition reaction of $CH_3M{\equiv}MCH_3$ (M=C, Si, Ge) with C_2H_4. The transition states and intermediates for the cycloaddition reaction have been found. The energy variation along the reaction

Electronic supplementary material The online version of this article (doi:10.1007/s00894-013-1882-0) contains supplementary material, which is available to authorized users.

S. Huo · X. Li (✉) · Y. Zeng · S. Zheng · L. Meng (✉)
College of Chemistry and Material Science, Hebei Normal University, Road East of 2nd Ring South, Shijiazhuang 050024, China
e-mail: lixiaoyan326@163.com
e-mail: menglp@hebtu.edu.cn

path, the relationship between the topological characteristic of density distribution are also discussed. The similarities and regularities of the three reactions of $CH_3M{\equiv}MCH_3$ (M=C, Si, Ge) with C_2H_4 have also been studied and compared. We expect that our computations will provide useful information for experimental synthesis and stimulate further studies.

Computation methods

The geometries of the reactants, transition states, intermediates, products and some points on the potential energy surface were located using MP2/6-311++G(d,p) [33] calculations with CCSD(T)/6-311++G(d,p) [34] energy corrections.Harmonic frequencies were calculated to characterize the stationary points and the reaction paths were traced out using intrinsic reaction coordinate (IRC) [35] in mass-weighted internal coordinates in both the forward and reverse directions from the transition state, with a step size equal to 0.01 $(amu)^{1/2}$ bohr. Computations were performed using the Gaussian 03 program package [36]. Molecular graphs of some points in the reactions were plotted according to the atoms in molecules (AIM) theory, as proposed by Bader [37, 38], using the program AIM2000 [39].

Results and discussion

Potential energy profiles on IRC paths

The geometry of the reactants, transition states, intermediates, and products of the $CH_3M{\equiv}MCH_3{+}C_2H_4$ (M=Si, C, and Ge) reaction on the potential energy surfaces have been optimized and are shown in Figs. 1 and S1–S2 (Supporting information), respectively. The potential energy profiles of these reactions are shown in Fig. 2. The relative energies of the reactants, transition states, intermediates, and products calculated at the CCSD(T) and MP2 levels are labeled in Fig. 2, too. For convenience, the energy of the reactants is set to be zero for reference and the CCSD(T) energies are used for the following discussion.

The reaction of $CH_3C{\equiv}CCH_3$ with C_2H_4 takes place as follows:

$$CH_3C{\equiv}CCH_3 + C_2H_4 \rightarrow Complex \xrightarrow{TS1} Int1 \xrightarrow{TS2} Int2 \xrightarrow{TS3} Product.$$

The pathway consists of four reaction steps. For the first step, a complex is formed between $CH_3C{\equiv}CCH_3$ and C_2H_4. The energy of the complex is 11.3 kJ mol^{-1} lower than that of the reactants. In the next step, the C(3) atom of $CH_3C{\equiv}CCH_3$ attacks the C(1) atom of C_2H_4 and, as the reaction proceeds, the distance between C(1) and C(3) continuously decreases. As the distances C(1)-C(3) decreases to 1.6594 Å, the reaction arrives at TS1. In TS1, the linear structure of $CH_3C{\equiv}CCH_3$ has changed to a trans-bent structure, in which the bond length of C(3)-C(4) has increased to 1.3214 Å. After TS1, the distance between C(1) and C(3) continues to decrease, so does the length of the C(2)-C(3) bond. When the bond lengths of C(1)-C(3), C(2)-(3) have reduced to 1.5772 Å and 1.5372 Å, respectively, Int1 forms. The decreasing bond lengths means that the C(1)-C(3) and C(2)-C(3) bonds strengthen. In the reaction process, a three-membered ring forms between the C(1), C(2) and C(3) atoms. The energy barrier of this step is 204.8 kJ mol^{-1}, which is the highest energy barrier along the whole pathway. Therefore, this step is the rate controlling step. Furthermore, the energy of Int1 is 155.4 kJ mol^{-1} higher than that of the complex, so this step is endothermic. The reaction barrier and the energy difference between the complex and Int1 determine that the reverse reaction is easier. Therefore,

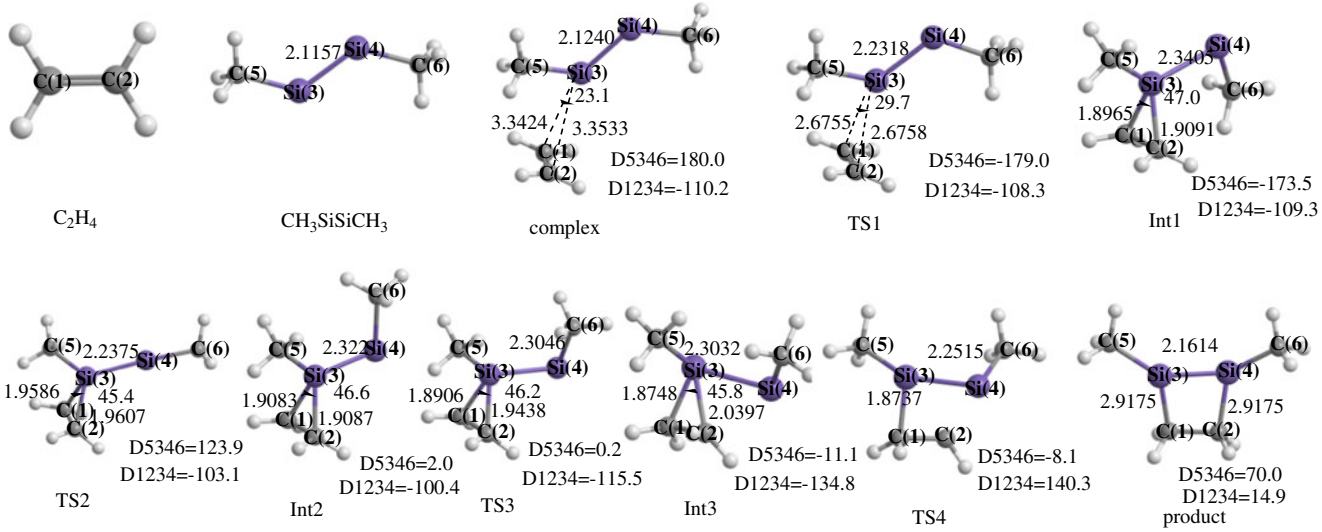

Fig. 1 Geometries of all stationary points of the $CH_3Si{\equiv}SiCH_3{+}C_2H_4$ reaction (bond lengths in Å, bond angles in degree)

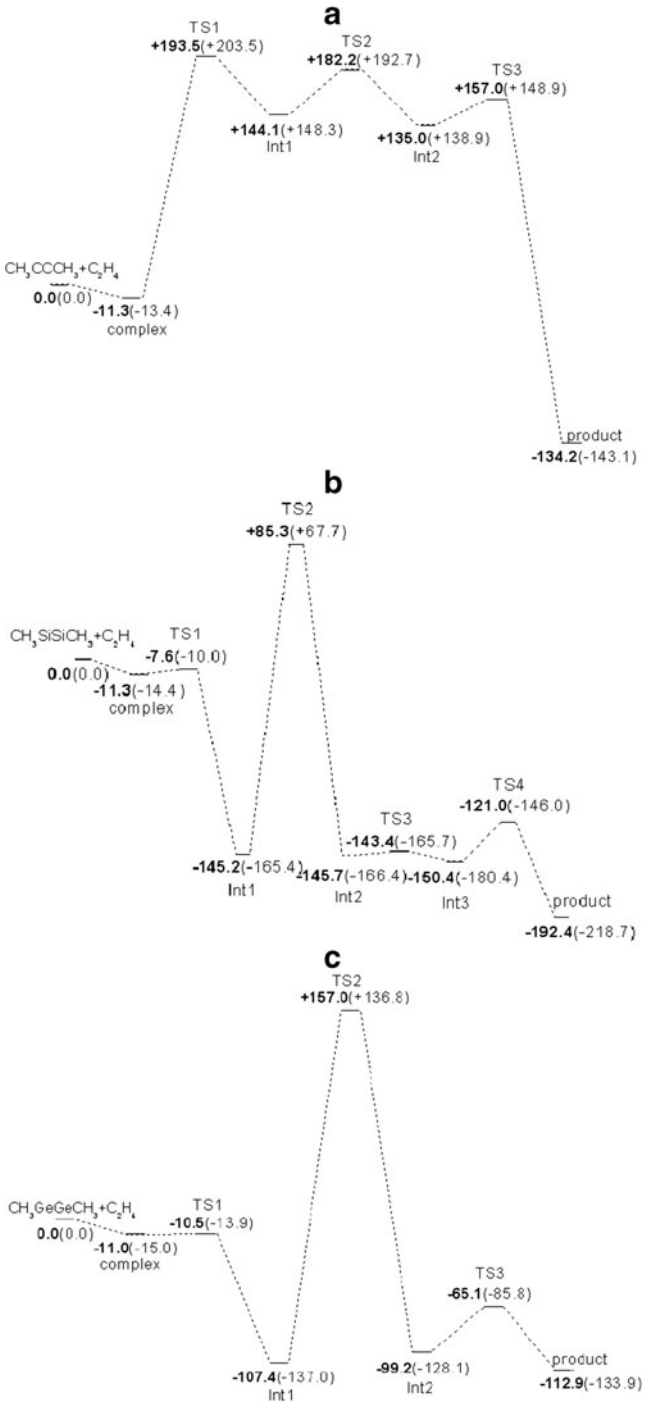

Fig. 2 Potential energy profiles for CH3M≡MCH3+C2H4 (M=(**a**)C, (**b**)Si, (**c**)Ge) reactions(CCSD(T) energy is bold typeface; the corresponding MP2energy is shown in brackets)

Int1 can revert easily to the complex. In total, the high energy barrier and reaction energy mean that the $CH_3C{\equiv}CCH_3{+}C_2H_4$ reaction occurs difficultly. The third step is an isomerization process of Int1 to Int2 *via* TS2. From Int1 to Int2, the C(1)-C(3) and C(2)-C(3) bond length show no obvious changes, neither does the bond angle C(1)-C(3)-C(2). However, changes of the dihedral angles C(5)-C(3)-C(4)-C(6) (D5346) are very clear throughout the isomerization process. From Int1 to Int2, D5346 changes from 168.1 ° to 1.6 °, which means that *trans*-$CH_3C{\equiv}CCH_3$ changes to *cis*-$CH_3C{\equiv}CCH_3$. The energy barrier of this step is only 38.1 kJ mol^{-1}, which means that the isomerization is easy. The three-membered ring is always present in the isomerization process. For the last step, the $CH_3C{\equiv}CCH_3$ rotates around the C(2)-C(3) bond, the C(1)-C(3) bond length continuously increases, then C(1)-C(3) bond disappears. In the proceeding of the reaction, the C(4), C(3), C(2) and C(1) atom come to the same plane, C(1) atom connects to C(4) atom and C(1)-C(4) bond forms. Hence, the C(1)-C(2)-C(3)-C(4) four-membered ring structure forms. The point group of the product is C_{2v}. The noticeable change of the dihedral angle D1234 can also illuminate the geometry changes. In Int2, D1234 is −100.3 °, then it decreases to −59.2 ° in TS3 and to zero in the product.

The $CH_3Si{\equiv}SiCH_3{+}C_2H_4$ reaction takes place as follows:

$$CH_3Si \equiv SiCH_3 + C_2H_4 \rightarrow Complex \overset{TS1}{\rightarrow} Int1 \overset{TS2}{\rightarrow} Int2 \overset{TS3}{\rightarrow} Int3 \overset{TS4}{\rightarrow} Product.$$

Firstly, a complex forms whose energy is 11.3 kJ mol^{-1} lower than that of the reactants. Secondly, the C(1)-Si(3) and C(2)-Si(3) bond lengths decrease to form Int1(*trans*-$CH_3SiSiCH_3$) *via* TS1. Thirdly, *trans*-$CH_3SiSiCH_3$ is isomerized to *cis*-$CH_3Si{\equiv}SiCH_3$. The next step is an additional step compared to the $CH_3CCCH_3{+}C_2H_4$ reaction. In this step, Int2 changes to Int3 with the dihedral angle C(1)-C(2)-Si(3)-Si(4) (D1234) changing from −100.4 ° to 134.8 °. Lastly, the product, which has C_2 symmetry, is produced. It is worth noticing that the $CH_3Si{\equiv}SiCH_3$ does not rotate like $CH_3C{\equiv}CCH_3$. In this process, the C(2)-Si(3) bond breaks and then C(2) atom links to Si(4) atom. Hence, a four-membered ring C(1)-C(2)-Si(4)-Si(3) forms. Although the reaction steps of $CH_3Si{\equiv}SiCH_3{+}C_2H_4$ are similar to those of $CH_3C{\equiv}CCH_3{+}C_2H_4$, the energy barriers are much less than for the same step in the $CH_3C{\equiv}CCH_3{+}C_2H_4$ reaction. The first energy barrier is 3.7 kJ mol^{-1}, so Int1 can form easily. The next step is the rate controlling step, whose energy barrier is 230.5 kJ mol^{-1}. Although this energy barrier is not low, the first step is an exothermic reaction and TS2 is only 85.3 kJ mol^{-1} higher than that of the reactants. Moreover, the energy of the product is −192.4 kJ mol^{-1} lower than that of the reactants, so the reaction of $CH_3Si{\equiv}SiCH_3{+}C_2H_4$ can proceed readily.

The reaction path of $CH_3Ge{\equiv}GeCH_3{+}C_2H_4$ reaction is

$$CH_3Ge{\equiv}GeCH_3 + C_2H_4 \rightarrow Complex \overset{TS1}{\rightarrow} Int1 \overset{TS2}{\rightarrow} Int2 \overset{TS3}{\rightarrow} Product.$$

Firstly, a complex yields. Next, the C(1) and C(2) atoms get closer to the Ge(3) atom and a C(1)-Ge(3)-C(2) three-membered ring forms. Then, the *trans*-$CH_3Ge{\equiv}GeCH_3$ is isomerized to *cis*-$CH_3Ge{\equiv}GeCH_3$. Finally, the C(1)-Ge(3)-C(2) three-membered ring disappears and a new C(1)-C(2)-Ge(4)-Ge(3) four-membered ring forms. The energy of TS2 is

157.0 kJ mol^{-1} higher than that of the reactants, and the total reaction is exothermic. The reaction energy is 112.9 kJ mol^{-1}, so the $CH_3Ge{\equiv}GeCH_3+C_2H_4$ reaction can also occur easily.

Comparing the three title reactions, the $CH_3Si{\equiv}SiCH_3+C_2H_4$ reaction has the highest reaction activity since it has the lowest energy barriers and the lowest energy of the product. The $CH_3Ge{\equiv}GeCH_3+C_2H_4$ reaction can also take place easily. The $CH_3C{\equiv}CCH_3+C_2H_4$ reaction occurs with difficulty because it has the highest energy barriers. The lowest reactivity of $CH_3C{\equiv}CCH_3+C_2H_4$ can be explained from the electronic structure. The heavier main-group element compounds (especially multiple bonded species) possess frontier orbitals with small energy separations, so they have high activity [27]. Therefore, the reactivity of $CH_3M{\equiv}MCH_3$ (M=Si and Ge) is much higher than $CH_3C{\equiv}CCH_3$ and the $CH_3C{\equiv}CCH_3+C_2H_4$ reaction occurs difficultly. Moreover, the work by Power [1] discovered that the $CH_3Si{\equiv}SiCH_3$ has a little more significant diradical character than $CH_3Ge{\equiv}GeCH_3$. The more significant diradical character, the higher reactivity of the compound. Thus, the reactivity of $CH_3Si{\equiv}SiCH_3$ is a little higher than that of $CH_3Ge{\equiv}GeCH_3$. In total, the reactivity of $CH_3E{\equiv}ECH_3$ with C_2H_4 increases form C to Si, but reduces from again from Si to Ge. The calculated results provide a reasonable explanation for the experimental results of Nagase [28] and Power et al. [29], that disilyne and digermyne can react readily with unsaturated molecules such as alkynes and azides under ambient conditions, and these results also mean that the reaction mechanisms of $CH_3M{\equiv}MCH_3+C_2H_4$ are similar to that of $RSi{\equiv}SiR$ ($R=Si^{i}Pr[CH(SiMe_3)_2]_2$)+2-butene reaction [28].

Topological structure changes along the IRC paths

Topological studies along the reaction paths can provide very useful information about the reaction [40]. According to Bader's AIM theory [37, 38, 41], two atoms are defined to be bonded if their atomic volumes share a common interatomic surface, and there is a bond critical point (BCP) on this surface. The electron density $\rho(r_c)$ at the BCP is used to describe the strength of a bond. The larger $\rho(r_c)$, the stronger the chemical bond. The existence of the ring critical point (RCP) indicates that a ring structure exists.

In order to discuss the chemical bond changes along the IRC path, a topological analysis of the electronic density was carried out at a number of points along the reaction paths. The molecular graphs along the IRC paths are displayed in Figs. 3 and S3, Supporting information. The topological characteristics at the bond critical point (BCP) and ring critical point (RCP) on the $CH_3M{\equiv}MCH_3+C_2H_4$ reaction pathway (1a: M=C; 1b: M=Si) are listed in Table SI, Supporting information. For the reaction $CH_3M{\equiv}MCH_3+C_2H_4$, we assigned S_1, S_2 and S_3 as reaction coordinates for the sequence complex→Int1, Int2→product(Int3), and Int3→product, respectively.

The topological characteristics along the $CH_3C{\equiv}CCH_3+C_2H_4$ reaction pathway are shown in Fig. S3, Supporting information. First, the C1 atom of the C_2H_4 attacks the C(3) atom of $CH_3C{\equiv}CCH_3$, C(1)-C(3) bond forms. After TS1, at S_1=+0.19, C(2)-C(3) bond forms, at this time, the C(1)-C(3) bond still exists, then C(1)-C(2)-C(3) three-membered ring forms. From S_1=+0.19 to TS2, the $\rho(r_c)$ at the BCP of C(2)-C(3) and C(1)-C(3) becomes larger and larger, which means that the C(2)-C(3) and C(1)-C(3) become stronger. After TS2, the $\rho(r_c)$ of C(1)-C(3) bond continues decreasing. After S_2=−0.05, the C(1)-C(3) bond breaks and the C(1)-C(2)-C(3) three-membered ring dissociates. Then with the C(4) atom rotating to C(1)C(2)C(3) plane, the C(1) atom connects C(3) atom again at S_2=+0.10. After that the C(1)-C(3) bond path slips along the C(3)-C(4) bond, then C(1) links to C(4) atom and the C(1)-C(2)-C(3) three-membered ring changes to the C(1)-C(2)-C(3)-C(4) four-membered ring structure. This means that the $CH_3C{\equiv}CCH_3+C_2H_4$ reaction is also a [2+1] cycloaddition, instead of a direct [2+2] cycloaddition.

The molecular graph of the $CH_3Si{\equiv}SiCH_3+C_2H_4$ reaction is shown in Fig. 3. As can be seen, a T-shaped conflict structure exists in the complex in which the Si(3) atom of $CH_3Si{\equiv}SiCH_3$ connects neither to the C(1) or C(2) atoms but to the BCP of the C(1)-C(2) bond (defined as B1). As the reaction proceeds, the electronic density $\rho(r_c)$ at BCP(Si(3)-B1) continually increases, which means that the interaction between $CH_3Si{\equiv}SiCH_3$ and C_2H_4 becomes stronger. As the reaction proceeds to S_1=+0.27, the bond path migrates from B1 to the C(2) atom of C_2H_4, then the C(2)-Si(3) bond forms. At S_1=+0.36, following the formation of the C(1)-Si(3) bond, the C(1)-Si(3)-C(2) three-membered ring structure first exists. From S_1=+0.36 to Int1, the $\rho(r_c)$ at the BCP of C(2)-Si(3) and C(1)-Si(3) becomes larger and larger. For the process Int1 to Int2, the $\rho(r_c)$ of all bonds show little change. The C(1)-Si(3)-C(2) three-membered ring structure exists until Int3. As the reaction proceeding, the C(2)-Si(3) bond becomes weaker and weaker, then at S_3=−0.35, a strange phenomenon occurs, in which the old C(1)-Si(3)-C(2) three-membered ring and a new three-membered ring C(2)-Si(3)-Si(4) coexist. At S_3=−0.28, the C(2)-Si(3) bond disappears and the two three-membered rings combine to give a new four-membered ring formed by the C(1), Si(3), Si(4) and C(2) atoms. Then the $\rho(r_c)$ at the BCP of C(1)-Si(3) bond decreases and that of C(2)-Si(4) increases, until they reach the same value, 0.1155, at the product. The molecular graph of the $CH_3Si{\equiv}SiCH_3+C_2H_4$ reaction shows that, in the initial step, a three-membered ring structure forms, then the three-membered ring structure changes to a four-membered ring structure. These topological changes mean that the reaction of $CH_3Si{\equiv}SiCH_3+C_2H_4$ is [2 +1] cycloaddition, instead of a direct [2+2] cycloaddition.

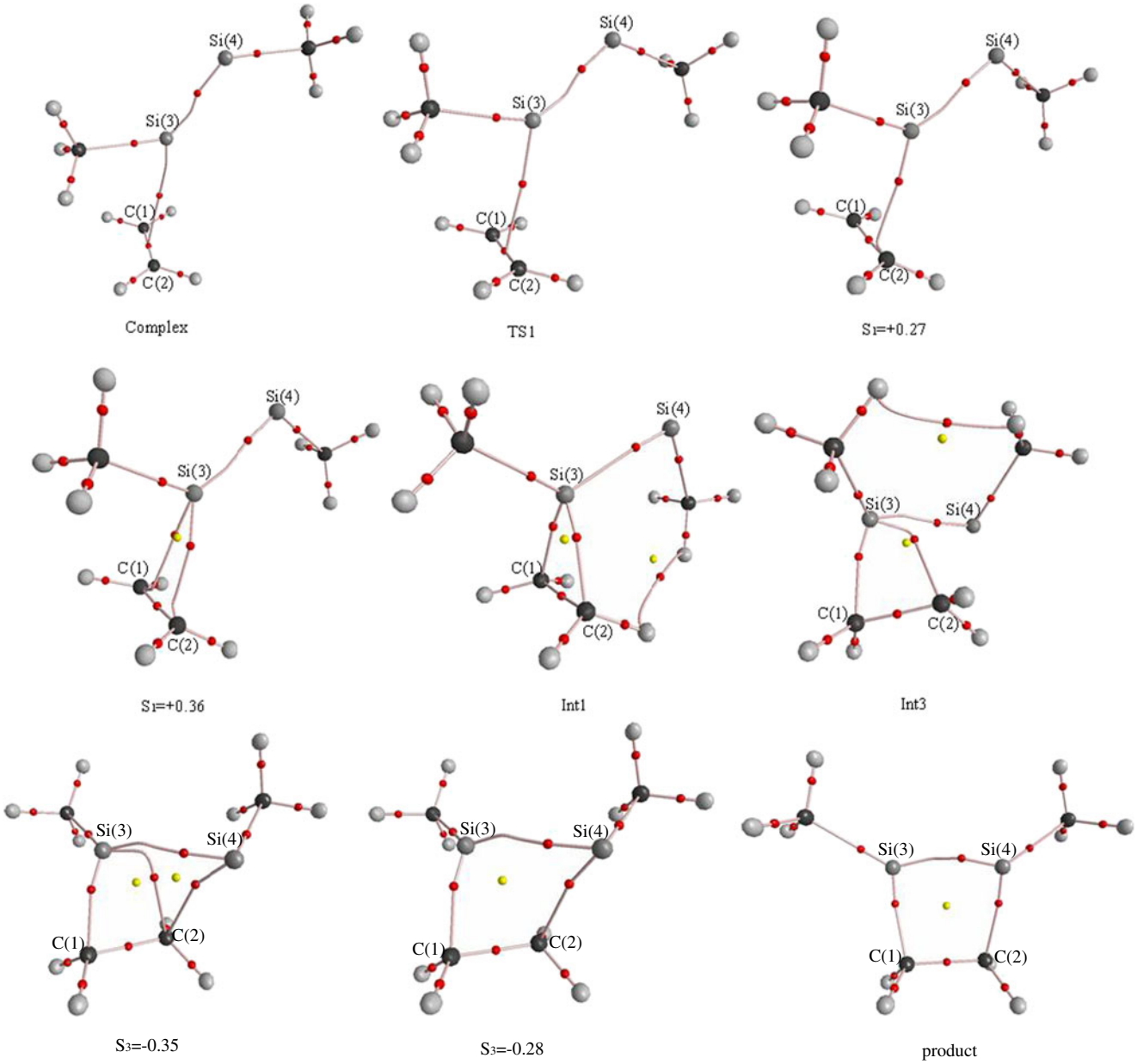

Fig. 3 Molecular graph along the $CH_3Si{\equiv}SiCH_3{+}C_2H_4$ reaction path (small ● represents bond critical point and small ● represents ring critical point)

Conclusions

The reaction mechanism of $CH_3M{\equiv}MCH_3$ (M=C, Si, Ge) with C_2H_4 is discussed using quantum chemical and topological techniques. The analyses carried out in this work lead to the following main conclusions:

(1) The reaction mechanisms of the title three reactions are similar. The reaction of $CH_3M{\equiv}MCH_3$ (M=C, Si, Ge) with C_2H_4 is a cycloaddition reaction, since four-numbered-ring structures exist in the products.

(2) Of the three titled reactions, the $CH_3Si{\equiv}SiCH_3{+}C_2H_4$ reaction has the highest reaction activity because it has the lowest energy barriers and the lowest energy for the product. The $CH_3C{\equiv}CCH_3{+}C_2H_4$ reaction occurs with difficulty since it has the highest energy barriers. The calculated results provide a reasonable explanation for the experimental results.

(3) The topological characteristics of the three titled reactions show that the $CH_3M{\equiv}MCH_3$ (M=C, Si, Ge)+C_2H_4 reactions involve, in the initial step, [2+1] cycloaddition, instead of a direct [2+2] cycloaddition.

Acknowledgments Thanks for International Science Editing to edit this paper. This work was supported by the National Natural Science Foundation of China (Contract NO. 21102033, 21171047, 21073051), the Natural Science Foundation of Hebei Province (Contract NO.

B2011205058), the Education Department Foundation of Hebei Province (NO. ZD2010126, ZH2012106).

References

1. Power PP (2007) Organmetallics 26:4362–4372
2. Luke BT, Peple JA, Krogh-Jespersen MB, Apeloig Y, Karni M, Chandrasekhar J, Schleyer PVR (1986) J Am Chem Soc 108:270–284
3. Koseki S, Gordon MS (1988) J Phys Chem 92:364–367
4. Golegrove BT, Schaefer HF III (1991) J Am Chem Soc 113:1557–1561
5. Kobayashi K, Nagase S (1997) Organometallic 16:2489–2491
6. Nagase S, Kobayashi K, Tagagi N (2000) J Organmet Chem 611:254–258
7. Karni M, Apeloig Y (2002) Silicon Chem 1:61–66
8. Pignedoli CA, Curioni A, Andreoni W (2005) Chem Phys Chem 6:1795–1799
9. Lein M, Krapp A, Frenking G (2005) J Am Chem Soc 127:6290–6299
10. Frenking G, Krapp A, Nagase S, Takagi N, Sekiguchi A (2006) Chem Phys Chem 7:799–800
11. Pignedoli CA, Curioni A, Andreoni W (2006) Chem Phys Chem 7:801–802
12. Jung Y, Brynda M, Power PP, Head-Gordon M (2006) J Am Chem Soc 128:7185–7192
13. Sekiguchi A, Zigler SS, West R, Michl J (1986) J Am Chem Soc 108:4241–4242
14. Cordonnier M, Bogey M, Demuynck C, Destombes J-L (1982) J Chem Phys 97:7984–7989
15. Bogey M, Bolvin H, Demuynck C, Destombes J-L (1991) Phys Rev Lett 66:413–416
16. Karni M, Apeloig Y, Schroder D, Zummack W, Rabezanna R, Schwarz H (1999) Angew Chem Int Ed 38:332–335
17. Pietschnig R, West R, Powell DR (2000) Organometallics 19:2724–2729
18. Power PP (1999) Chem Rev 99:3463–3503
19. Pu L, Twamley B, Power PP (2000) J Am Chem Soc 122:3524–3525
20. Phillips AD, Wright RJ, Olmstead MM, Power PP (2002) J Am Chem Soc 124:5930–5931
21. Pu L, Phillips AD, Richards AF, Stender M, Simons RS, Olmstead MM, Power PP (2003) J Am Chem Soc 125:11626–11636
22. Sekiguchi A, Kinjo R, Ichinohe M (2004) Science 305:1755–1757
23. Sugiyama Y, Sasamori T, Hosoi Y, Furukawa Y, Takagi N, Nagase S, Tokitoh N (2006) J Am Chem Soc 128:1023–1031
24. Fischer RC, Pu L, Fettinger JC, Brynda MA, Power PP (2006) J Am Chem Soc 128:11366–11367
25. Wiberg N, Vasisht SK, Fischer G, Mayer P (2004) Z Anorg Allg Chem 630:1823–1828
26. Stender M, Phillips AD, Wright RJ, Power PP (2002) Angew Chem Int Ed 41:1785–1787
27. Power PP (2010) Nature 463:171–177
28. Kinjo R, Ichinohe M, Sekiguchi A, Takagi N, Sumimoto M, Nagase S (2007) J Am Chem Soc 129:7766–7767
29. Cui C, Olmstead MM, Power PP (2004) J Am Chem Soc 126:5062–5063
30. Cui C, Brynda M, Olmstead MM, Power PP (2004) J Am Chem Soc 126:6510–6511
31. Glowacki DR, Marsden SP, Pilling MJ (2009) J Am Chem Soc 131:13896–13897
32. Kına A, Piecuch P (2006) J Phys Chem A 110:367–378
33. Head-Gordon M, Pople JA, Frisch MJ (1988) Chem Phys Lett 153:503–506
34. Scuseria GE, Schaefer HF III (1989) J Chem Phys 90:3700–3703
35. Ishida G, Morokuma K, Komornicki A (1977) J Chem Phys 66:2153–2156
36. Frisch MJ, Trucks GW, Schlegel HB *et al* (2004) GAUSSIAN 03, Revision D. 02. Gaussian, Inc, Wallingford
37. Bader RFW (1990) Atoms in molecules: a quantum theory. Clarendon, Oxford
38. Popelier P (2000) Atoms in molecules-an introduction. UMIST Manchester
39. Biegler-könig F, Schonbohm J (2000) AIM 2000 program package, ver. 2.0. University of Applied Science, Bielefeld
40. Alikhani ME (1997) Chem Phys Lett 277:239–244
41. Bader RFW (1991) Chem Rev 91:893–928